Article

Electrochemical Switching of a Fluorescent Molecular Rotor Embedded within a Bistable Rotaxane

Yilei Wu, Marco Frasconi, Wei-Guang Liu, Ryan M. Young, William A. Goddard, Michael R. Wasielewski, and J. Fraser Stoddart

Just Accepted

Electrochemical Switching of a Fluorescent

Molecular Rotor Embedded within a Bistable Rotaxane

Yilei Wu,[†] Marco Frasconi,*,[§] Wei-Guang Liu,[‡] Ryan M. Young,[†] William A. Goddard III,[‡]

Michael R. Wasielewski*,[†,∥] and J. Fraser Stoddart*,[†, Δ,⊥]

[†]*Department of Chemistry and* [∥]*Institute for Sustainability and Energy at Northwestern (ISEN), Northwestern University, 2145, Sheridan Road, Evanston, Illinois 60208, United States*

[§]*Department of Chemical Sciences, University of Padova, Via Marzolo 1, Padova 35131, Italy*

[‡]*Materials and Process Simulation Center, California Institute of Technology, Pasadena, California 91125, United States*

[Δ] *Institute for Molecular Design and Synthesis, Tianjin University, 92 Weijin Road, Nankai District, Tianjin 300072, China*

[⊥]*School of Chemistry, University of New South Wales, Sydney, NSW 2052, Australia*

*Correspondence Addresses

Professor Marco Frasconi
Department of Chemical Sciences
University of Padova
Via Marzolo 1, Padova 35131, Italy
Email: marco.frasconi@unipd.it

Professor Michael R. Wasielewski
Department of Chemistry and Institute for Sustainability and Energy at
Northwestern (ISEN), Northwestern University
2145 Sheridan Road, Evanston, IL 60208-3113 (USA)
Fax: (+1)-847-467-1425
Email: m-wasielewski@northwestern.edu

Professor J. Fraser Stoddart
Department of Chemistry
Northwestern University
2145 Sheridan Road, Evanston, IL 60802-3113 (USA)
Fax: (+1)-847-491-1009
Email: stoddart@northwestern.edu

ABSTRACT: We report how the nanoconfined environment, introduced by the mechanical bonds within an electrochemically switchable bistable [2]rotaxane, controls the rotation of a fluorescent molecular rotor, namely an 8-phenyl-substituted boron dipyrromethene (BODIPY). The electrochemical switching of the bistable [2]rotaxane induces changes in the ground-state co-conformation and in the corresponding excited-state properties of the BODIPY rotor. In the starting redox state, when no external potential is applied, the cyclobis(paraquat-*p*-phenylene) (CBPQT^{4+}) ring component encircles the tetrathiafulvalene (TTF) unit on the dumbbell component, leaving the BODIPY rotor unhindered and exhibiting low fluorescence. Upon oxidation of the TTF unit to a TTF^{2+} dication the CBPQT^{4+} ring is forced toward the molecular rotor leading to an increased energy barrier for the excited-state to rotate the rotor into the state with the high non-radiative rate constant, resulting in an overall 3.4-fold fluorescent enhancement. On the other hand, when the solvent polarity is high enough to stabilize the excited charge transfer state between the BODIPY rotor and the CBPQT^{4+} ring, the movement of the ring towards the BODIPY rotor produces an unexpectedly strong fluorescent signal decrease as the result of the photoinduced electron transfer from the BODIPY rotor to the CBPQT^{4+} ring. The nanoconfinement effect introduced by mechanical bonding can effectively lead to the modulation of the physicochemical properties as observed in this bistable [2]rotaxane. On account of the straightforward synthetic strategy and the facile modulation of switchable electrochromic behavior, our approach could pave the way for the development of new stimuli-responsive materials based on mechanically interlocked molecules for future electro-optical applications, such as sensors, molecular memories and molecular logic gates.

INTRODUCTION

Molecular devices and machines are of considerable interest on account of their potential use in sensing, catalytic, electronics, and nanotechnological applications.[1] Mechanically interlocked molecules (MIMs) constitute promising nanoscale molecular assemblies for the development of switches,[2] actuators,[3] ratchets[4] and motors.[5] Well-known examples are bistable [2]rotaxanes,[2a,6]

which are MIMs comprising a ring component mechanically bonded onto a linear dumbbell component with two (or more) recognition sites for occupation by the ring component. The ability to manipulate reversibly the relative positioning of the ring component with respect to the dumbbell component is crucial to exploring their use in operating molecular devices. The controlled rotary movement of the ring component around the dumbbell has been achieved[7] by introducing suitable steric hindrance between the two components of the rotaxane. On the other hand, the net linear translation of the ring with respect to a constitutionally asymmetric axle has been demonstrated in molecular shuttles[4b,c] and pseudorotaxanes[8] by exploiting ratchet mechanisms.[9] Recently, a rotaxane-based molecular shuttle, combined with an overcrowded alkene rotary motor, has led to the transformation of the unidirectional rotation of the molecular motor into a reciprocating shuttling motion,[10] thus coupling rotary and translational movements in a MIM. Indeed, rotary motors are a class of molecular machines that display controlled rotation of one component with respect to the other around single[11] or double[12] bonds driven, for the most part, by either light or heat.

Fluorescent molecular rotors are compounds whose photoluminescence is modulated by segmental mobility (twisting)—that is, the locally excited (LE) electronic state can relax either by (i) the radiative emission of a photon or by (ii) the formation of a "dark state" that relaxes non-radiatively to the ground state (GS) on account of internal rotation.[13] If the local environment around the fluorophore permits rapid internal rotation in the excited state, fast non-radiative decay processes can effectively quench its fluorescence. On the other hand, any environmental restriction to twisting in the excited state because of free volume, molecular crowding or solvent viscosity, slows down rotational relaxation, enhancing fluorescence efficiency from the LE state. This environmental sensitivity of fluorescent molecular rotors has been exploited[13] extensively in biological applications to probe, in real time, local microviscosity in biofluids and biomembranes. One of the most widely used[14] fluorescent molecular rotors is (**Scheme 1a**) the BODIPY-rotor. The introduction of steric constrains in the form of substituents onto the phenyl ring or the dipyrrin units of the BODIPY is an effective approach to increasing the quantum yield of these rotors by

preventing free rotation of the phenyl group, thus reducing loss of energy from the excited states via non-radiative molecular motions.[15] Indeed, a theoretical study shows[15a] that the phenyl ring rotation and accompanying boron-dippyrin distortions allow access to an excited-state conformation with low radiative probability and facile nonradiative deactivation to the ground state, thereby limiting the fluorescence yields of the dyes. Such a distorted conformation is energetically inaccessible in a system bearing the sterically hindered o-tolyl or mesityl group, leading to a high radiative probability—and high fluorescence quantum yield—involving conformations at or near the initial Franck-Condon form of the excited state.[15b] An increase in the fluorescence quantum yield of BODIPY-rotor is also observed[14] by increasing the solvent viscosity, that results in the restricted rotation of the phenyl group, thus preventing non-radiative relaxation. This property of the BODIPY-rotor and its derivatives has been employed successfully to measure viscosity in model lipid membranes,[16] in protocells,[17] and in the inner membranes of living cells.[18] One of the main advantages of BODIPY-rotor over other reported molecular rotors is the wide dynamic range of its fluorescence response,[14] corresponding to a broad range of viscosities, and a very weak sensitivity to solvent polarity[19] and temperature.[16] The control of the rotation of a fluorescent molecular rotor, imposed by mechanical bonds within the nanoconfinement[20] provided by a MIM, however, has not been explored so far to the best of our knowledge.

Herein, we have designed (**Scheme 1b**) and synthesized a novel electrochemically switchable bistable [2]rotaxane (**6^{4+}**) with an embedded fluorescent rotor where the fluorescence output is actuated by an electrochemical stimulus. The bistable [2]rotaxane (**6^{4+}**) is formed between the π-electron-poor cyclobis(paraquat-p-phenylene) $CBPQT^{4+}$ ring, and a dumbbell containing a π-electron-rich tetrathiafulvalene (TTF) unit with a fluorescent BODIPY rotor, acting as a stopper. This particular bistable [2]rotaxane has only one switchable recognition unit and therefore exists as one translational co-conformation in its ground state. Upon complete oxidation of the TTF unit to the stable, doubly charged TTF^{2+} dication, the $CBPQT^{4+}$ ring is forced into juxtaposition with the BODIPY rotor, as a result of Coulombic repulsions. The nature of the switching process has been investigated using (i) 1-D and 2-D NMR spectroscopy, (ii) steady-state and ultrafast time-

resolved spectroscopy, (iii) electrochemical experiments and (iv) quantum mechanical calculations. In low polarity solvents—e.g. PhMe—the oxidation of the TTF unit to a TTF^{2+} dication drives the $CBPQT^{4+}$ ring towards the BODIPY rotor, increasing the fluorescence quantum yield of the latter. This remarkable fluorescent enhancement is the consequence of the increased energy barrier associated with its excited-state rotation which is responsible for its high non-radiative rate constant. The novelty of our approach lies in the ability to control the rotation of a molecular rotor by the constrained nanoconfined[20] environment introduced by the mechanical bonding associated with this electrochemically switchable bistable [2]rotaxane (**Scheme 1b**). The bistable [2]rotaxane can therefore be considered as a model electromechanical *molecular brake* based on Coulombic repulsion and actuated by redox inputs where the co-conformational change is readily monitored through the fluorescence output. On the other hand, in high polarity solvents—e.g. MeCN—an excited charge-shifted (CS) state involving electron transfer from the BODIPY rotor to the $CBPQT^{4+}$ ring become energetically accessible, enforcing association between the two components and, hence, decreasing the fluorescence output of the BODIPY rotor. The ultrafast, photoinduced electron transfer from the BODIPY rotor to the $CBPQT^{4+}$ ring in MeCN is corroborated by femtosecond transient absorption (fsTA) spectroscopy, which reveals the characteristic absorption features of the reduced $CBPQT^{4+}$ ring. The unconventional electrochromic behavior of the fluorescent molecular rotor embedded within this bistable [2]rotaxane, generated by the mechanical motion of the redox-actuated switching process, demonstrates that mechanical bonding remains a powerful strategy to create unpredictable emergent properties in MIMs through the induced nanoconfinement effect. This electrochemically addressable fluorescent-bistable rotaxane is of particular interest for the development of electro-optical applications because, in contrast with conventional electro-optical molecule switches, the change in the fluorescence output in the rotaxane-based system is modulated by the mechanical movement within the MIM which can lead to more sophisticated outcomes.

RESULTS AND DISCUSSION

Synthesis and NMR Spectroscopy. The 1,3-dipolar cycloadditions[21] of azides with alkynes, otherwise known as the copper-catalyzed azide-alkyne cycloaddition (CuAAC) approach to synthesis, has been demonstrated[22] to be highly effective when employed in the final step, leading to the formation of mechanical bonds in the syntheses of MIMs, such as rotaxanes. The CuAAC reaction occurs readily under very mild conditions and at room temperature, a quality that is desirable for the template-directed synthesis of MIMs on account of the optimal stabilization of the supramolecular intermediates.

TTF and its derivatives have been used widely in the design and synthesis of reversible, electrochemically switchable, supramolecular systems[23] and MIMs.[24,25] The π-electron-rich neutral state has the ability to be oxidized reversibly, not just once but twice at mild potentials to give a stable radical cation and dication, respectively. In its neutral state, the TTF unit is bound strongly[23a] inside the π-electron-poor $CBPQT^{4+}$. Oxidation, however, leads to the ejection of the oxidized TTF^{2+} dication from inside the tetracationic cyclophane as a consequence of Coulombic repulsions.

The BODIPY-alkyne **4**, which was synthesized following a method reported in the literature by Wagner and Lindsey[26], was obtained (**Scheme 2**) in four steps. As for the synthesis of the *meso*-substituted dipyrromethanes **2**, we adopted a one-flask synthesis, which was developed previously for the preparation of *trans*-substituted porphyrins.[27] Pyrroles readily undergo acid-catalyzed condensation at room temperature in presence of highly electrophilic carbonyl compounds, such as the aldehyde **1**, which is used to form the *meso*-bridge.[28] In order to avoid oligomerization, a large excess of pyrrole is employed. Moreover, pyrrole serves as the solvent for the reaction, leading to the direct formation of the dipyrromethane **2**.

The π-electron-rich TTF derivative **5** was prepared using a previously reported procedure.[29] Upon mixing of **5** with 1 molar equiv of CBPQT•4PF$_6$ in Me$_2$CO, the solution immediately turns in to an intense emerald-green color, indicating the formation of a donor-acceptor pseudorotaxane complex—namely, [**5** ⊂ CBPQT]•4PF$_6$. Reaction with tetrakis(acetonitrile) copper(I)

hexafluorophosphate in presence of the tris[(1-benzyl-1H-1,2,3-triazol-4-yl)methyl]amine (TBTA) at 20 °C for 5 days promoted the desired click reaction, affording the bistable [2]rotaxane **6**•4PF$_6$ as a dark green solid in 20% yield. Similarly, the reference dumbbell compound **DB** was obtained (Scheme 2) under similar reaction condition in the absence of **CBPQT**•4PF$_6$. The molecular structures and compound purities were ascertained by mass spectrometry and HPLC, as well as by 1-D and 2-D NMR spectroscopy. See the Supporting Information (SI) for detailed synthetic procedures and characterization.

The ^{1}H NMR spectrum (**Figure 1**) of **6**•4PF$_6$ confirms its mechanically interlocked nature and the fact that the CBPQT^{4+} ring encircles the TTF unit in the ground state. Notably, the separation of the signals for both the α- and β-bipyridinium protons on the CBPQT^{4+} ring is observed at room temperature. This observation is to be expected, as the constitutional asymmetry of the dumbbell component imposes its lack of symmetry on the CBPQT^{4+} ring, rendering the α- and β-bipyridinium protons heterotopic and thus, in each case, giving rise to separate signals. We were not able to observe (**Figure S8**, Supporting Information) any ground-state shuttling by dynamic ^{1}H NMR spectroscopy, within the temperature range from 238 to 308 K, indicating that the CBPQT^{4+} ring resides, to all intents and purposes, solely on the TTF unit, at least within the limits of detection provided by variable-temperature ^{1}H NMR spectroscopy. This observation is consistent with the one-station nature of the bistable [2]rotaxane when the TTF unit is neutral.

The bistable [2]rotaxane **6**•4PF$_6$ can be actuated (**Scheme 1**) by chemical oxidation of **6**$^{4+}$ to **6**$^{6+}$ in CD$_3$CN using 2 equiv of tris(4-bromophenyl)ammoniumyl hexachloroantimonate as an oxidizing agent.[30] The effects of chemical switching can be monitored by ^{1}H NMR spectroscopy, steady-state UV-Vis absorption and emission spectroscopy. The ^{1}H NMR spectrum (**Figure 2**) is characterized by a substantial change, as a consequence of large downfield shifts of the TTF^{2+} proton resonances, as well as those associated with the neighboring methylene groups. These changes are in agreement with previously reported[31] spectroscopic data. Before the oxidation, the spectrum of the bistable rotaxane **6**$^{4+}$ reveals two pairs of peaks of almost equal integration (56:44) at δ = 6.19 and 6.14 ppm, and δ = 6.02 and 5.98 ppm, which can be assigned to the constitutionally

heterotopic TTF methine protons in the *cis* and *trans* isomers, respectively. These isomers are in dynamic equilibrium on the laboratory timescale. Following oxidation, the signals for the constitutionally heterotopic methine protons on the TTF^{2+} dication resonate[32] at δ = 9.30 and 9.17 ppm, while those associated with the methylene protons on the adjacent CH_2 groups are shifted downfield to 5.21 and 4.96 ppm. In this oxidized state, *cis-trans* isomerism is removed since the TTF^{2+} dication is no longer planar.[30a] The movement of the $CBPQT^{4+}$ ring from the TTF unit to the BODIPY rotor was probed (**Figures S9** and **S10**) by two-dimensional (2D) Nuclear Overhauser Effect (NOE) measurements, where the presence of through-space correlations between the resonances for the BODIPY protons and those on the $CBPQT^{4+}$ ring in $\mathbf{6}^{6+}$ were observed. It should be noted that the interaction between the $CBPQT^{4+}$ ring and the BODIPY rotor was absent in the reduced $\mathbf{6}^{4+}$ state. The disappearance of NOE correlations between the methylene protons next to the TTF unit and those of the $CBPQT^{4+}$ ring corroborates the switching to $\mathbf{6}^{6+}$. Upon treatment with Zn dust, the TTF^{2+} was reduced (**Figure 2**) to its neutral form and the $CBPQT^{4+}$ ring moved back to reside on the π-electron-rich TTF unit, as indicated by the ^{1}H NMR spectrum of the product, in order to re-establish the CT interactions between the TTF and the $CBPQT^{4+}$ ring.

Steady-State UV/Vis Spectroscopy. The UV/Vis absorption spectrum (**Figure 3a**, green trace) of the bistable [2]rotaxane $\mathbf{6}\cdot 4PF_6$ shows the characteristic charge transfer (CT) absorption band[33] centered on 843 nm (ε = 3500 $M^{-1}cm^{-1}$) for the TTF unit residing inside the $CBPQT^{4+}$ ring. Furthermore, in the visible region, the strong absorption band at 499 nm (ε = 48000 $M^{-1}cm^{-1}$), typical of an $S_1 \leftarrow S_0$ electronic transition of BODIPY chromophore unit, is observed. The UV region is characterized by the $S_2 \leftarrow S_0$ transition of BODIPY (376 nm, ε = 16000 $M^{-1}cm^{-1}$) and the $CBPQT^{4+}$ absorption at 260 nm (ε = 40000 $M^{-1}cm^{-1}$). Switching of $\mathbf{6}^{4+}$ was investigated in a 6.25 μM solution of the $4PF_6^-$ salt in MeCN when $Fe(ClO_4)_3$ was added.[34] Addition of 1 mol equiv of this chemical oxidant led (**Figure 3a**, orange trace) to disappearance of the CT absorption band at 843 nm and the rise of absorption bands centered on 450 and 600 nm characteristic[35] of the mono-oxidized form of the TTF. Further addition of the oxidant (up to 2 mol equiv) led the disappearance of the absorption bands for the mono-oxidized TTF unit and the enhancement of

the band at 375 nm (**Figure 3b**, red trace), indicative[35] of TTF^{2+} dication formation. Notably, the movement of the $CBPQT^{4+}$ ring away from the TTF unit is also accompanied by a small red-shift of the absorption maxima of BODIPY from 499 to 505 nm. This observed ground-state electronic perturbation is most likely caused by the enforced encirclement of the BODIPY rotor by the tetracationic cyclophane as the reference **DB** does not show (**Figure 3c,d**) any red-shift upon oxidation of the TTF unit. After the reduction with Zn powder, the original spectrum is quantitatively restored. In summary, both the ^{1}H NMR spectroscopic and UV/Vis spectrophotometric experiments showed clearly that the redox switching of the TTF unit forces the $CBPQT^{4+}$ ring toward and away from the BODIPY rotor.

Electrochemistry. The switching of the bistable [2]rotaxane can also be enacted electrochemically. The $CBPQT^{4+}$ ring shows (**Figure 4a**) two characteristic reversible two-electron reductions with $E_{1/2}$ at –270 and –715 mV *vs* Ag/AgCl while the BODIPY rotor reveals (**Figure 4b**) a reversible one-electron reduction at $E_{1/2}$ = –652 mV and an irreversible oxidation peak at +1630 mV. The TTF oxidation processes, that are $TTF \rightarrow TTF^{•+}$ followed by $TTF^{•+} \rightarrow TTF^{2+}$ one-electron events, are well-resolved in the CV of **DB** (**Figure 4c**) with $E_{1/2}$ at +392 and +755 mV, respectively. On the other hand, the oxidative scan of the bistable [2]rotaxane **6•4PF$_6$** (**Figure 4d**) shows only one peak centered at +772 mV encompassing both of the one-electron processes which together generate the TTF^{2+} dicationic state from its neutral form to the radical $TTF^{•+}$ intermediate. The complete disappearance of the first oxidation peak matches the fact that the TTF unit within the bistable [2]rotaxane **6•4PF$_6$** is encircled completely by the electron poor $CBPQT^{4+}$ ring, such that the first TTF oxidation is shifted substantially to more positive potentials, close to the potential for the second oxidation.[13] We also performed variable scan-rate CV measurements in order to elucidate the kinetics associated with the return of the $CBPQT^{4+}$ ring from the oxidation-induced co-conformation to the ground-state co-conformation (GSCC). As observed in other bistable MIMs,[24e] the initial oxidation of the TTF unit forces the $CBPQT^{4+}$ ring onto the alternative recognition site and the subsequent re-reduction of the TTF unit back to its neutral form does not result immediately in the regeneration of the GSCC. The transient co-

conformation, where the CBPQT^{4+} ring still encircles the weaker binding site, while the TTF unit is back in the neutral state, is referred to as the metastable-state co-conformation (MSCC). As the conversion of the MSCC to the GSCC is usually an activated process, its kinetics have a measurable rate, from seconds to hours, which depends on the nature of the linker, the temperature and the environment.[31] In case of the bistable [2]rotaxane **6**$^{4+}$, however, even at high scan rate (2000 mV/s, **Figure S11**), we could not detect any presence of the MSCC, which would appear as emergence of the first oxidation of free TTF in the second scan. The absence of any detectable MSCC suggests that there is not much, if any, affinity between CBPQT^{4+} ring and BODIPY rotor and their dissociation after the oxidation step is driven largely by the Coulombic repulsion between the tetracationic cyclophane and the TTF^{2+} dication.

Quantum Mechanical Calculations. In order to examine the energetics that govern the intramolecular noncovalent bonding interactions in the bistable [2]rotaxane **6**•4PF$_6$ in its different redox states, we performed density functional theory (DFT) calculations at the M06-2X/6-311++G**//M06-2X/6-31G* level that includes corrections for van der Waals attraction (normally not included in DFT).[36] Although **6**$^{4+}$ has multiple rotatable C–O and C–C single bonds, we started with the linear conformation that has the longest possible distance between the TTF at the center and two ends of **6**$^{4+}$. This minimizes the electrostatic repulsion between TTF^{2+} and CBPQT^{4+} once TTF is oxidized and CBPQT^{4+} is driven to the two ends. We assume that the entropic contribution to the free energy from the multiple rotatable single bonds will cancel out as CBPQT^{4+} relocates. The ground-state geometries and energy landscapes predicted from the DFT methods (**Figure 5**), carried out on the **6**$^{4+}$ and **6**$^{6+}$ states, are in agreement with the experimental observations. In **6**$^{4+}$ the CBPQT^{4+} ring prefers to reside on the TTF unit rather than on the BODIPY rotor by 19.8 kcal/mol due to stronger donor-acceptor interactions between CBPQT^{4+} and TTF. Once two electrons are removed from the TTF unit, the strong electrostatic repulsion between TTF^{2+} and CBPQT^{4+} drives the CBPQT^{4+} ring to relocate preferentially beside the BODIPY rotor leading to 47.9 kcal/mol energy stabilization. The other co-conformation of **6**$^{6+}$ has the CBPQT^{4+} ring move to the di-*t*-butyl benzene unit, which is 10.0 kcal/mol higher in energy than when the CBPQT^{4+}

ring resides beside the BODIPY rotor.

Redox Modulation of Excited-State Properties. In order to demonstrate the ability of the bistable [2]rotaxane to modulate fluorescence outputs and excited-state dynamics on the BODIPY rotor, we performed steady-state fluorescence titration and fsTA measurements before and after chemical oxidation. A dilute solution of **6**•4PF$_6$ in PhMe excited at 467 nm shows (**Figure 6a**, green trace) the characteristic emission spectra of BODIPY around 515 nm. The measured fluorescence quantum yield is low (Φ_{em} = 0.19 %) and insensitive to the solvent polarity, as observed (**Figure 6b** and **6c**, green traces) in both MeCN and THF. These results are consistent[37] with those reported for sterically unhindered BODIPY derivatives. Upon addition of 2 mol equiv of Fe(ClO$_4$)$_3$, a 3.4-fold increase in fluorescence intensity was observed for **6**$^{6+}$ in PhMe. For comparison, the fluorescence signal of the BODIPY unit in the reference dumbbell **DB**, measured (**Figure S12**) before and after oxidation of the TTF unit, does not show appreciable fluorescence changes in the tested solvents. We attribute the fluorescence signal enhancement present in the oxidized bistable [2]rotaxane to the expected increase in energy barrier for the intramolecular rotation of BODIPY rotor induced by the enforced positioning of the CBPQT^{4+} ring close to the rotor in the **6**$^{6+}$ state. Unexpectedly, when the same fluorescence titration experiment of the bistable [2]rotaxane is performed in the MeCN (**Figure 6c**), a nearly 3-fold decrease in the fluorescence quantum yield is observed. In THF (**Figure 6b**), which has an intermediate polarity compared to PhMe and MeCN, neither an increase nor a decrease in the fluorescence signal is observed upon addition of Fe(ClO$_4$)$_3$. The different fluorescence response of [2]rotaxane **6**•4PF$_6$, upon chemical switching in the three solvents, suggests that an additional excited state reaction, which is highly sensitive to the solvent polarity, must be involved. We hypothesize that the quenching of fluorescence in MeCN could be indicative of a photoinduced electron transfer reaction from the BODIPY singlet excited state to the electron accepting CBPQT^{4+} ring. In order to obtain support for this hypothesis, we performed fsTA spectroscopy investigations.

Photoexcitation of the bistable [2]rotaxane **6**•4PF$_6$ in MeCN at 497 nm with a 150 fs laser pulse populated the lowest excited singlet state of the BODIPY rotor, which displays a prominent

ground-state bleach (GSB) at 500 nm, and which overlaps partially with stimulated emission (SE) signals in the 500–600 region (**Figure 7a**). These transient features decay bi-exponentially with time constants of $\tau_{S1*\to S1} = 4.1 \pm 0.3$ ps and $\tau_{S1\to S0} = 31.7 \pm 0.6$ ps. The first decay component can be assigned to the solvation evolution or vibrational/conformational relaxation associated with BODIPY-core in the excited state, while the relaxed excited singlet state decays with the slower time constant to the ground state. On the other hand, photoexcitation of the oxidized [2]rotaxane 6^{6+} under the same conditions generates ^{1}*BODIPY, which decays rapidly ($\tau_{CS} = 1.4 \pm 0.3$ ps) to produce (**Figure 7c**) a new species with an absorption maximum at 610 nm that is indicative[38] of the presence of the CBPQT$^{3+\bullet}$ (**Figure S13**). The free energy change for such process in polar MeCN can be estimated as $\Delta G_{CS} = e(E_{OX} - E_{RED}) - E_S$, where E_{OX} is the oxidation potential (+1.69 V, **Figure 4**) of the BODIPY rotor and E_{RED} is the reduction potential (–0.27 V, **Figure 4**) of the CBPQT^{4+}, while E_S is the energy of ^{1}*BODIPY (+2.44 eV, from the average of absorption and fluorescence maxima), so that $\Delta G_{CS} = -0.51$ eV, and is thus consistent with the observed fluorescence quenching results. The ΔG_{IP} for the formation of an ion pair in a solvent of arbitrary polarity can be determined by using an expression developed by Weller:[39]

$$\Delta G_{IP} = e(E_{OX} - E_{RED}) + \frac{3e^2}{4\pi\varepsilon_0\varepsilon_s r_{12}} + \frac{e^2}{4\pi\varepsilon_0}\left(\frac{1}{2r_D} + \frac{1}{2r_A}\right)\left(\frac{1}{\epsilon_s} - \frac{1}{\epsilon_{sp}}\right) \qquad (1)$$

where the redox potentials are measured in a high polarity solvent with a static dielectric constant ε_{sp}, e is the charge of the electron, r_{12} is the ion pair distance, r_D and r_A are the ionic radii, and ε_s is the static dielectric constant of a solvent of arbitrary polarity. While the term involving the ion pair distance is the Coulombic interaction of the ions, the last term accounts for the lesser ability of the lower polarity solvents to stabilize charges as compared to the higher polarity used in the electrochemical measurements. However, there are several limitations with this treatment for estimating ΔG_{IP} for large π-stacked donor−acceptor systems. First, the ionic radii of the donor and acceptor are larger than the distance between them, which violates the assumption of a hard-sphere model surrounded by a continuous dielectric that is intrinsic to eq 1. Second, the BODIPY unit is highly shielded from the surrounding medium by the presence of the CBPQT^{4+} ring; thus,

BODIPY experiences a significant electrostatic influence from the $CBPQT^{4+}$ ring, which will deviate from that of the bulk solvent. Nevertheless, one can estimate that the energy of CS state is destabilized by at least 0.6 eV in PhMe relative to its energy in MeCN, making the photoinduced electron transfer reaction endoenergetic by ≥ 0.1 eV.[40] Notably, the charge recombination proceeds biexponentially. The shorter lifetime (8.0 ± 0.3 ps) can be safely assigned to the geminate recombination from TTF- $CBPQT^{3+\bullet}$-$BODIPY^{+\bullet}$ to the ground state. A smaller fraction of the population, however, can undergo to a charge-shift reaction to generate $TTF^{+\bullet}$- $CBPQT^{4+}$-$BODIPY^{+\bullet}$, which ultimately decays in 1644 ± 87 ps. The energy levels and excited state decay pathways under various conditions are summarized in **Figure 8**.

CONCLUSIONS

We have reported the synthesis of an electrochemically switchable bistable [2]rotaxane with an embedded fluorescent molecular rotor—the BODIPY rotor—and demonstrated that the redox actuation of this mechanically interlocked molecule can impose a nanoconfined constrained environment that controls the rotation of the fluorescent rotor, resulting in a unique electrochromic effect. The electrochemically switchable [2]rotaxane, $6 \bullet 4PF_6$, composed of a $CBPQT^{4+}$ ring mechanically interlocked with a dumbbell component containing a TTF recognition site and a functional fluorescent molecular rotor in the form of a BODIPY stopper, was synthetized in good yield by a template-directed protocol utilizing a "threading-followed-by-stoppering" approach, in combination with the CuAAC reaction. The bistable [2]rotaxane can be switched reversibly so that the $CBPQT^{4+}$ ring is positioned next to the BODIPY rotor upon oxidation of TTF unit to its TTF^{2+} dication. We have investigated the switching of the ground state co-conformation by means of 1-D and 2-D NMR spectroscopies and investigated the corresponding electronic excited state dynamics changes using a variety of steady-state and time-resolved optical spectroscopies. Remarkably, two completely different mechanisms of fluorescence co-exist within this fluorescent-bistable rotaxane upon the switching of its ground state co-conformation; (i) fluorescence enhancement by reducing the loss of energy from the excited states to the non-

radiative molecular motions of the BODIPY-rotor in low polarity solvents and (ii) fluorescence quenching on account of the photoinduced electron transfer reaction from the BODIPY singlet excited state to the electron accepting $CBPQT^{4+}$ ring in polar solvents. This unconventional electrochromic effect is generated by the constrained nanoconfined environment introduced by the mechanical bond in this electrochemically switchable bistable [2]rotaxane which imparts the forced association between the $CBPQT^{4+}$ ring and the BODIPY rotor driven purely by the Coulombic repulsion between the tetracationic ring and the TTF^{2+} dication on the dumbbell. We believe that the extension of the concept of the nanoconfinement effect,[20] introduced by mechanical binding in the context of stimuli-responsive materials based on MIMs, could lead to novel electro-optical switchable materials that can perform complex operations, holding the promise for future applications as sensors, molecular memories and molecular logic gates.

■ ASSOCIATED CONTENT

Supporting Information

The Supporting Information is available free of charge on the ACS Publications website.

Experimental details, including synthesis, NMR, and supportive figures; Additional electrochemical studies and fluorescence spectra; quantum mechanical calculations.

■ AUTHOR INFORMATION

Corresponding Authors

marco.frasconi@unipd.it; m-wasielewski@northwestern.edu; stoddart@northwestern.edu

Notes

The authors declare no competing financial interest.

■ ACKNOWLEDGMENTS

■ REFERENCES

(1) (a) Sauvage, J.-P. Transition Metal-Containing Rotaxanes and Catenanes in Motion: Toward Molecular Machines and Motors. *Acc. Chem. Res.* **1998**, *31*, 611–619. (b) Balzani, V.; Credi, A.; Raymo, F. M.; Stoddart, J. F. Artificial Molecular Machines. *Angew Chem., Int. Ed.* **2000**, *39*, 3349−3391. (c) Browne, W. R.; Feringa, B. L. Making Molecular Machines Work. *Nature Nanotechnol.* **2006**, *1*, 25−35. (d) Kay, E. R.; Leigh, D. A.; Zerbetto, F. Synthetic Molecular Motors and Mechanical Machines. *Angew. Chem., Int. Ed.* **2007**, *46*, 72−191. (e) Cacialli, F.; Wilson, J. S.; Michels, J. J.; Daniel, C.; Silva. C.; Friend, R. H.; Severin, N.; Samorì, P.; Rabe, J. P.; O'Connell, M. J.; Taylor, P. N.; Anderson, H. L. Cyclodextrin-Threaded Conjugated Polyrotaxanes as Insulated Molecular Wires with Reduced Interstrand Interactions. *Nat Mater.* **2002**, *1*, 160−164. (f) Langton, M. J.; Beer, P. D. Rotaxane and Catenane Host Structures for Sensing Charged Guest Species. *Acc. Chem. Res.* **2014**, *47*, 1935−1949. (g) De Bo, G.; Gall, M. A. Y.; Kuschel, S.; De Winter, J.; Gerbaux, P.; Leigh, D. A. An Artificial Molecular Machine that Builds an Asymmetric Catalyst. *Nature Nanotech.* **2018**, *13*, 381−385. (h) Chen S.; Wang Y.; Nie T.; Bao C.; Wang C.; Xu T.; Lin Q.; Qu DH.; Gong X.; Yang Y.; Zhu L.; Tian H. An Artificial Molecular Shuttle Operates in Lipid Bilayers for Ion Transport. *J. Am. Chem. Soc.* **2018**, *140*, 17992−17998. (i) Corra, S.; de Vet, C.; Groppi, J.; La Rosa, M.; Silvi, S.; Baroncini, M.; Credi, A. Chemical On/Off Switching of Mechanically Planar Chirality and Chiral Anion Recognition in a [2]Rotaxane Molecular Shuttle. *J. Am. Chem. Soc.* **2019**, *141*, 9129−9133.

(2) (a) Bruns, C. J.; Stoddart, J. F. *The Nature of the Mechanical Bond: From Molecules to Machines*; Wiley: New York, 2017. (b) Stoddart, J. F. Mechanically Interlocked Molecules (MIMs) Molecular Shuttles, Switches, and Machines (Nobel Lecture). *Angew. Chem., Int. Ed.*

2017, *56*, 11094−11125.

(3) Liu, Y.; Flood, A. H.; Bonvallett, P. A.; Vignon, S. A.; Northrop, B. H.; Tseng, H. R.; Jeppesen, J. O.; Huang, T. J.; Brough, B.; Baller, M.; Magonov, S.; Solares, S. D.; Goddard, III W. A.; Ho, C. M.; Stoddart, J. F. Linear Artificial Molecular Muscles. *J. Am. Chem. Soc.* **2005**, *127*, 9745−9759.

(4) (a) Serreli, V.; Lee, C. F.; Kay, E. R.; Leigh, D. A. A Molecular Information Ratchet. *Nature* **2007**, *445*, 523−527. (b) Alvarez-Pérez, M.; Goldup, S. M.; Leigh, D. A.; Slawin, A. M. Z. A Chemically-Driven Molecular Information Ratchet. *J. Am. Chem. Soc.* **2008**, *130*, 1836–1838. (c) Carlone, A.; Goldup, S. M.; Lebrasseur, N.; Leigh, D. A.; Wilson, A. A Three-Compartment Chemically-Driven Molecular Information Ratchet. *J. Am. Chem. Soc.* **2012**, *134*, 8321−8323.

(5) (a) Koumura, N.; Zijlstra, R. W. J.; Van Delden, R. A.; Harada, N.; Feringa, B. L. Light-Driven Monodirectional Molecular Rotor. *Nature* **1999**, *401*, 152–155. (b) Leigh, D. A.; Wong, J. K. Y.; Dehez, F.; Zerbetto, F. Unidirectional Rotation in a Mechanically Interlocked Molecular Rotor. *Nature* **2003**, *424*, 174–179; (c) Wilson, M. R.; Solá, J.; Carlone, A.; Goldup, S. M.; Lebrasseur, N.; Leigh, D. A. An Autonomous Chemically Fuelled Small-Molecule Motor. *Nature* **2016**, 534, 235−240. (d) Kassem, S.; van Leeuwen, T.; Lubbe, A. S.; Wilson, M. R.; Feringa, B. L.; Leigh, D. A. Artificial Molecular Motors. *Chem. Soc. Rev.* **2017**, *46*, 2592–2621.

(6) (a) Bissell, R. A.; Córdova, E.; Kaifer, A. E.; Stoddart, J. F. A Chemically and Electrochemically Switchable Molecular Shuttle. *Nature* **1994**, *369*, 133−137. (b) Anelli, P.-L.; Asakawa, M.; Ashton, P. R.; Bissell, R. A.; Clavier, G.; Górski, R.; Kaifer, A. E.; Langford, S. J.; Mattersteig, G.; Menzer, S.; Philp, D.; Slawin, A. M. Z.; Spencer, N.; Stoddart, J. F.; Tolley, M. S.; Williams, D. Toward Controllable Molecular Shuttles. J. *Chem. Eur. J.* **1997**, *3*, 1113–1135. (c) Durola, F.; Sauvage, J.-P. Fast Electrochemically Induced Translation of the Ring in a Copper-Complexed [2]Rotaxane: The Biisoquinoline Effect. *Angew. Chem. Int. Ed.* **2007**, *46*, 3537–3540. (d) Nygaard, S.; Leung, K. C.-F.; Aprahamian, I.; Ikeda, T.; Saha, S.; Laursen, B. W.; Kim, S.-Y.; Hansen, S. W.; Stein, P. C.; Flood, A. H.; Stoddart, J. F.; Jeppesen, J. O. Functionally Rigid Bistable [2]Rotaxanes. *J. Am. Chem. Soc.* **2007**, *129*, 960–970. (e) Andersen, S.S.; Share, A. I.; Poulsen, B. L.; Kørner, M.; Duedal, T.; Benson, C. R.; Hansen, S. W.; Jeppesen, J. O.; Flood, A. H. Mechanistic Evaluation of Motion in Redox-Driven Rotaxanes Reveals Longer Linkers Hasten Forward Escapes and Hinder Backward

Translations. *J. Am. Chem. Soc.* **2014**, *136*, 6373–6384.

(7) (a) Nishimura, D.; Oshikiri, T.; Takashima, Y.; Hashidzume, A.; Yamaguchi, H.; Harada, A. Relative Rotational Motion between α-Cyclodextrin Derivatives and a Stiff Axle Molecule. *J. Org. Chem.* **2008**, *73*, 2496–2502. (b) Yamauchi, K.; Miyawaki, A.; Takashima, Y.; Yamaguchi, H.; Harada, A. A Molecular Reel: Shuttling of a Rotor by Tumbling of a Macrocycle. *J. Org. Chem.* **2010**, *75*, 1040–1046. (c) Wang, Z.; Takashima, Y.; Yamaguchi, H.; Harada, A. Photoresponsive Formation of Pseudo[2]Rotaxane with Cyclodextrin Derivatives. *Org. Lett.* **2011**, *13*, 4356–4359.

(8) (a) Baroncini, M.; Silvi, S.; Venturi, M.; Credi, A. Photoactivated Directionally Controlled Transit of a Non-Symmetric Molecular Axle Through a Macrocycle. *Angew. Chem. Int. Ed.* **2012**, *51*, 4223–4226. (b) Li, H.; Cheng, C.; McGonigal, P. R.; Fahrenbach, A. C.; Frasconi, M.; Liu, W.-G.; Zhu, Z.; Zhao, Y.; Ke, C. F.; Lei, J. Y.; Young, R. M.; Dyar, S. M.; Co, D. T.; Yang, Y. W.; Botros, Y. Y.; Goddard, W. A., III; Wasielewski, M. R.; Astumian, R. D.; Stoddart, J. F. Relative Unidirectional Translation in an Artificial Molecular Assembly Fueled by Light. *J. Am. Chem. Soc.* **2013**, *135*, 18609–18620. (c) Ragazzon, G.; Baroncini, M.; Silvi, S.; Venturi, M.; Credi, A. Light-Powered Autonomous and Directional Molecular Motion of a Dissipative Self-Assembling System. *Nat. Nanotechnol.* **2015**, *10*, 70–75.

(9) (a) Astumian, R. D.; Derényi, I. Fluctuation Driven Transport and Models of Molecular Motors and Pumps. *Eur. Biophys. J.* **1998**, *27*, 474–489. (b) Pezzato, C.; Cheng, C.; Stoddart, J. F.; Astumian. R. D. Mastering the Non-Equilibrium Assembly and Operation of Molecular Machines. *Chem. Soc. Rev.* **2017**, *46*, 5491–5507.

(10) Yu, J.-J.; Zhao, L.-Y.; Shi, Z.-T.; Zhang, Q.; London, G.; Liang, W.-J.; Gao, C.; Li, M.-M.; Cao, X.-M.; Tian, H.; Feringa, B. L.; Qu, D.-H. Pumping a Ring-Sliding Molecular Motion by a Light-Powered Molecular Motor. *J. Org. Chem.* **2019**, *84*, 5790–5802.

(11) (a) Kelly, T. R.; De Silva, H.; Silva, R. A. Unidirectional Rotary Motion in a Molecular System. *Nature* **1999**, *401*, 150–152. (b) Fletcher, S. P.; Dumur, F.; Pollard, M. M.; Feringa, B. L. A Reversible, Unidirectional Molecular Rotary Motor Driven by Chemical Energy. *Science* **2005**, *310*, 80–82.

(12) (a) Koumura, N.; Zijlstra, R. W. J.; van Delden, R. A.; Harada, N.; Feringa, B. L. Light-Driven Monodirectional Molecular Rotor. *Nature* **1999**, *401*, 152–155. (b) Wang, J. B.; Feringa, B. L. Dynamic Control of Chiral Space in a Catalytic Asymmetric Reaction Using a Molecular

Motor. *Science* **2011**, *331*, 1429–1432. For a review see: (c) Feringa, B. L. The Art of Building Small: From Molecular Switches to Molecular Motors. *J. Org. Chem.* **2007**, *72*, 6635– 6652.

(13) For reviews on fluorescent molecular rotors see: (a) Haidekker, M. A.; Theodorakis, E. A. Molecular Rotors—Fluorescent Biosensors for Viscosity and Flow. *Org. Biomol. Chem.* **2007**, *5*, 1669–1678. (b) Kuimova, M. K. Mapping Viscosity in Cells Using Molecular Rotors. *Phys. Chem. Chem. Phys.* **2012**, *14*, 12671–12686. (c) Lee, S. C.; Heo, J.; Woo, H. C.; Lee, J. A.; Seo, Y. H.; Lee, C. L.; Kim, S.; Kwon, O. P. Fluorescent Molecular Rotors for Viscosity Sensors. *Chem. - Eur. J.* **2018**, *24*, 13706–13718.

(14) Kuimova, M. K.; Yahioglu, G.; Levitt, J. A.; Suhling, K. Molecular Rotor Measures Viscosity of Live Cells via Fluorescence Lifetime Imaging. *J. Am. Chem. Soc.* **2008**, *130*, 6672–6673.

(15) (a) Li, F.; Yang, S. I.; Ciringh, Y.; Seth, J.; Martin, C. H., III; Singh, D. L.; Kim, D.; Birge, R. R.; Bocian, D. F.; Holten, D.; Lindsey, J. S. Design, Synthesis, and Photodynamics of Light-Harvesting Arrays Comprised of a Porphyrin and One, Two, or Eight Boron-Dipyrrin Accessory Pigments. *J. Am. Chem. Soc.* **1998**, *120*, 10001−10017. (b) Kee, H. L.; Kirmaier, C.; Yu, L. H.; Thamyongkit, P.; Youngblood, W. J.; Calder, M. E.; Ramos, L.; Noll, B. C.; Bocian, D. F.; Scheidt, W. R.; Birge, R. R.; Lindsey, J. S.; Holten, D. Structural Control of the Photodynamics of Boron-Dipyrrin Complexes. *J. Phys. Chem. B* **2005**, *109*, 20433–20443.

(16) Wu, Y. L.; Stefl, M.; Olzynska, A.; Hof, M.; Yahioglu, G.; Yip, P.; Casey, D. R.; Ces, O.; Humpolickova, J.; Kuimova, M. K. Molecular Rheometry: Direct Determination of Viscosity in L-o and L-d Lipid Phases via Fluorescence Lifetime Imaging. *Phys. Chem. Chem. Phys.* **2013**, *15*, 14986–14993.

(17) Tang, T. Y. D.; Hak, C. R. C.; Thompson, A. J.; Kuimova, M. K.; Williams, D. S.; Perriman, A. W.; Mann, S. Fatty Acid Membrane Assembly on Coacervate Microdroplets as a Step Towards a Hybrid Protocell Model. *Nat. Chem.* **2014**, *6*, 527–533.

(18) Lopez-Duarte, I.; Vu, T. T.; Izquierdo, M. A.; Bull, J. A.; Kuimova, M. K. A Molecular Rotor for Measuring Viscosity in Plasma Membranes of Live Cells. *Chem. Commun.* **2014**, *50*, 5282–5284.

(19) Levitt, J. A.; Chung, P. H.; Kuimova, M. K.; Yahioglu, G.; Wang, Y.; Qu, J. L.; Suhling, K. Fluorescence Anisotropy of Molecular Rotors. *ChemPhysChem* **2011**, *12*, 662–672.

(20) Grommet, A. B.; Feller, M.; Klajn, R. Chemical Reactivity Under Nanoconfinement. *Nat. Nanotechnol.* **2020**, *15*, 256–271.

(21) (a) Huisgen, R. 1,3-Dipolar Cycloadditions. Past and Future. *Angew. Chem. Int. Ed.* **1963**, *2*, 565–598. (b) Rostovtsev, V. V.; Green, L. G.; Fokin, V. V.; Sharpless, K. B. A Stepwise Huisgen Cycloaddition Process: Copper(I)-Catalyzed Regioselective "Ligation" of Azides and Terminal Alkynes. *Angew. Chem. Int. Ed.* **2002**, *41*, 2596–2599. (c) Meldal, M.; Tornøe, C. W. Cu-Catalyzed Azide−Alkyne Cycloaddition. *Chem. Rev.* **2008**, *108*, 2952–3015.

(22) (a) Dichtel, W. R.; Miljanić, O. Š.; Spruell, J. M.; Heath, J. R.; Stoddart, J. F. Efficient Templated Synthesis of Donor−Acceptor Rotaxanes Using Click Chemistry. *J. Am. Chem. Soc.* **2006**, *128*, 10388–10390. (b) Dichtel, W. R.; Miljanić, O. Š.; Zhang, W.; Spruell, J. M.; Patel, K.; Aprahamian, I; Heath, J. R.; Stoddart, J. F. Kinetic and Thermodynamic Approaches for the Efficient Formation of Mechanical Bonds. *Acc. Chem. Res.* **2008**, *41*, 1750–1761; (c) Hänni, K. D.; Leigh, D. A. The Application of CuAAC 'Click' Chemistry to Catenane and Rotaxane Synthesis. *Chem. Soc. Rev.* **2010**, *39*, 1240–1251.

(23)(a) Jeppesen, J. O.; Nielsen, M. B.; Becher, J. Tetrathiafulvalene Cyclophanes and Cage Molecules. *Chem. Rev.* **2004**, *104*, 5115−5131. (b) Ziganshina, A. Y.; Ko, Y. H.; Jeona, W. S.; Kim, K. Stable π-Dimer of a Tetrathiafulvalene Cation Radical Encapsulated in the Cavity of Cucurbit[8]Uril. *Chem. Commun.* **2004**, 806−807. (c) Yoshizawa, M.; Kumazawa, K.; Fujita, M. Room-Temperature and Solution-State Observation of the Mixed-Valence Cation Radical Dimer of Tetrathiafulvalene, $[(TTF)_2]^{+\bullet}$, within a Self-Assembled Cage. *J. Am. Chem. Soc.* **2005**, *127*, 13456−13457. (d) Canevet, D.; Sallé, M.; Zhang, G.; Zhang, D.; Zhu, D. Tetrathiafulvalene (TTF) Derivatives: Key Building-Blocks for Switchable Processes. *Chem. Commun.* **2009**, 2245−2269. (d) Kim, D. S.; Chang, J.; Leem, S.; Park, J. S.; Thordarson, P.; Sessler, J. L. Redox- and pH-Responsive Orthogonal Supramolecular Self-Assembly: An Ensemble Displaying Molecular Switching Characteristics. *J. Am. Chem. Soc.* **2015**, *137*, 16038–16042. (e) Park, J. S.; Sessler, J. L. Tetrathiafulvalene (TTF)-Annulated Calix[4]pyrroles: Chemically Switchable Systems with Encodable Allosteric Recognition and Logic Gate Functions. *Acc. Chem. Res.* **2018**, *51*, 10, 2400−2410.

(24)(a) Asakawa, M.; Ashton, P. R.; Balzani ,V.; Credi, A.; Hamers, C.; Mattersteig, G.; Montalti, M.; Shipway, A. N.; Spencer, N.; Stoddart, J. F.; Tolley, M. S.; Venturi, M.; White, A. J. P.; Williams, D. J. A Chemically and Electrochemically Switchable [2]Catenane Incorporating a Tetrathiafulvalene Unit. *Angew. Chem. Int. Ed.* **1998**, *37*, 333–337. (b) Jeppesen, J. O.; Perkins, J.; Becher, J.; Stoddart, J. F. Slow Shuttling in an Amphiphilic Bistable [2]Rotaxane Incorporating a Tetrathiafulvalene Unit. *Angew. Chem. Int. Ed.* **2001**, *40*, 1216–1221. (c) Aprahamian, I.; Olsen, J. C.; Trabolsi, A.; Stoddart, J. F. Tetrathiafulvalene Radical Cation

Dimerization in a Bistable Tripodal [4]Rotaxane. *Chem. Eur. J.* **2008**, *14*, 3889–3895. (d) Wang, C.; Dyer, S. M.; Cao, D.; Fahrenbach, A. C.; Horwitz, N.; Colvin, M. T.; Carmieli, R.; Stern, C. L.; Dey, S. K.; Wasielewski, M. R.; Stoddart, J. F. Tetrathiafulvalene Hetero Radical Cation Dimerization in a Redox-Active [2]Catenane. *J. Am. Chem. Soc.* **2012**, *134*, 46, 19136– 19145. (e) Fahrenbach, A. C.; Bruns, C. J.; Cao, D.; Stoddart, J. F. Ground-State Thermodynamics of Bistable Redox-Active Donor–Acceptor Mechanically Interlocked Molecules. *Acc. Chem. Res.* **2012**, *45*, 1581–1592.

(25) (a) Spruell, J. M.; Coskun, A.; Friedman, D. C.; Forgan, R. S.; Sarjeant, A. A.; Trabolsi, A.; Fahrenbach, A. C.; Barin, G.; Paxton, W. F.; Dey, S. K.; Olson, M. A.; Benítez, D.; Tkatchouk, E.; Colvin, M. T.; Carmielli, R.; Caldwell, S. T.; Rosair, G. M.; Gunatilaka Hewage, S.; Duclairoir, F.; Seymour, J. L.; Slawin, A. M. Z.; Goddard, III, W. A.; Wasielewski, M. R.; Cooke, G.; Stoddart, J. F. Highly Stable Tetrathiafulvalene Radical Dimers in [3]Catenanes. *Nat. Chem.* **2010**, *2*, 870−879. (b) Frasconi, M.; Kikuchi, T.; Cao, D.; Wu, Y.; Liu, W.-G.; Dyar, S. M.; Barin, G.; Sarjeant, A. A.; Stern, C. L.; Carmieli, R.; Wang, C.; Wasielewski, M. R.; Goddard, III W. A.; Stoddart, J. F. Mechanical Bonds and Topological Effects in Radical Dimer Stabilization. *J. Am. Chem. Soc.* **2014**, *136*, 11011–11026.

(26) Wagner, R. W.; Lindsey, J. S. Boron-Dipyrromethene Dyes for Incorporation in Synthetic Multi-Pigment Light-Harvesting Arrays. *Pure Appl. Chem.* **1996**, *68*, 1373–1380.

(27) Lee, C.-H.; Lindsey, J. S. One-Flask Synthesis of Meso-Substituted Dipyrromethanes and their Application in the Synthesis of Trans-Substituted Porphyrin Building Blocks. *Tetrahedron* **1994**, *50*, 11427–11440.

(28) Lindsey, J. S.; Schreiman, I. C.; Hsu, H. C.; Kearney, P. C.; Marguerettaz, A. M. Rothemund and Adler-Longo Reactions Revisited: Synthesis of Tetraphenylporphyrins Under Equilibrium Conditions. *J. Org. Chem.* **1987**, *52*, 827–836.

(29) Avellini, T.; Li, H.; Coskun, A.; Barin, G.; Trabolsi, A.; Basuray, A. N.; Dey, S. K.; Credi, A.; Silvi, S.; Stoddart, J. F.; Venturi, M. Photoinduced Memory Effect in a Redox Controllable Bistable Mechanical Molecular Switch. *Angew. Chem. Int. Ed.* **2012**, *51*, 1611–1615.

(30) For a description of the oxidizing agent, tris(4-bromophenyl)ammoniumyl hexachloroantimonate, and its used in spectroscopic investigations, see: (a) Tseng, H.-R.; Vignon, S. A.; Stoddart, J. F. Toward Chemically Controlled Nanoscale Molecular Machinery. *Angew. Chem. Int. Ed.* **2003**, *42*, 1491–1495. For a review on this and other chemical oxidants commonly use in

NMR spectroscopic investigations, see: (b) Connelly, N. G.; Geiger, W. E. Chemical Redox Agents for Organometallic Chemistry. *Chem. Rev.* **1996**, *96*, 877–910.

(31) Spruell, J. M.; Paxton, W. F.; Olsen, J.-C.; Benítez, D.; Tkatchouk, E.; Stern, C. L.; Trabolsi, A.; Friedman, D. C.; Goddard, III W. A.; Stoddart, J. F. A Push-Button Molecular Switch. *J. Am. Chem. Soc.* **2009**, *131*, 11571–11580.

(32) Ashton, P. R.; Balzani, V.; Becher, J.; Credi, A.; Fyfe, M. C. T.; Mattersteig, G.; Menzer, S.; Nielsen, M. B.; Raymo, F. M.; Stoddart, J. F.; Venturi, M.; Williams, D. J. A Three-Pole Supramolecular Switch. *J. Am. Chem. Soc.* **1999**, *121*, 3951–3957.

(33) Asakawa, M.; Ashton, P. R.; Balzani, V.; Credi, A.; Mattersteig, G.; Matthews, O. A.; Montalti, M.; Spencer, N.; Stoddart, J. F.; Venturi, M. Electrochemically Induced Molecular Motions in Pseudorotaxanes: a Case of Dual Mode (Oxidative and Reductive) Dethreading. *Chem. - Eur. J.* **1997**, *3*, 1992–1996.

(34) The chemical oxidant $Fe(ClO_4)_3$ was chosen for the UV/Vis spectroscopic studies because it does not show any significant optical absorption band in the visible region, making changes in UV/Vis absorption spectra easier to interpret.

(35) Hünig, S.; Kiesslich, G.; Quast, H.; Scheutzow, D. Über Zweistufige Redoxsysteme, X1) Tetrathio‑Äthylene und Ihre Höheren Oxidationsstufen. *Liebigs Ann. Chem.* **1973**, 310–323.

(36) Zhao, Y.; Truhlar, D. G. The M06 Suite of Density Functionals for Main Group Thermochemistry, Thermochemical Kinetics, Noncovalent Interactions, Excited States, and Transition Elements: Two New Functionals and Systematic Testing of Four M06-Class Functionals and 12 Other Functionals. *Theor. Chem. Acc.* **2008**, *120*, 215–241.

(37) (a) Li, F. R.; Yang, S. I.; Ciringh, Y. Z.; Seth, J.; Martin, C. H.; Singh, D. L.; Kim, D. H.; Birge, R. R.; Bocian, D. F.; Holten, D.; Lindsey, J. S. Design, Synthesis, and Photodynamics of Light-Harvesting Arrays Comprised of a Porphyrin and One, Two, or Eight Boron-Dipyrrin Accessory Pigments. *J. Am. Chem. Soc.* **1998**, *120*, 10001–10017. (b) Alamiry, M. A. H.; Benniston, A. C.; Copley, G.; Elliott, K. J.; Harriman, A.; Stewart, B.; Zhi, Y. G. A Molecular Rotor Based on an Unhindered Boron Dipyrromethene (Bodipy) Dye. *Chem. Mater.* **2008**, *20*, 4024–4032. (c) Levitt, J. A.; Kuimova, M. K.; Yahioglu, G.; Chung, P. H.; Suhling, K.; Phillips, D. Membrane-Bound Molecular Rotors Measure Viscosity in Live Cells via Fluorescence Lifetime Imaging. *J. Phys. Chem. C* **2009**, *113*, 11634–11642.

(38) (a) Barnes, J. C.; Frasconi, M.; Young, R. M.; Khdary, N. H.; Liu, W. G.; Dyar, S. M.;

McGonigal, P. R.; Gibbs-Hall, I. C.; Diercks, C. S.; Sarjeant, A. A.; Stern, C. L.; Goddard, III W. A.; Wasielewski, M. R.; Stoddart, J. F. Solid-State Characterization and Photoinduced Intramolecular Electron Transfer in a Nanoconfined Octacationic Homo[2]Catenane. *J. Am. Chem. Soc.* **2014**, *136*, 10569–10572. (b) Fernando, I. R.; Frasconi, M.; Wu, Y.; Liu, W. G.; Wasielewski, M. R.; Goddard, III W. A.; Stoddart, J. F. Sliding-Ring Catenanes. *J. Am. Chem. Soc.* **2016**, *138*, 10214–10225.

(39) (a) Weller, A. Z. Photoinduced Electron Transfer in Solution: Exciplex and Radical Ion Pair Formation Free Enthalpies and their Solvent Dependence. *Phys. Chem.* **1982**, *133*, 93–98. (b) Young, R. M.; Dyar, S. M.; Barnes, J. C.; Juricek, M.; Stoddart, J. F.; Co, D. T.; Wasielewski, M. R. Ultrafast Conformational Dynamics of Electron Transfer in ExBox^{4+} ⊂ Perylene. *J. Phys. Chem. A* **2013**, *117*, 12438–12448.

(40) Complementary fsTA measurements in PhMe, in an attempt to corroborate the excited state dynamics, were unsuccessful because of the low solubility of both **6**•4PF$_6$ and **6**•6PF$_6$ in low polarity solvents. Additional efforts to tune the polarity have been made using a binary solvent mixture of PhMe and MeCN (90:10 vol/vol). The fluorescence spectra, resulting from carrying out a titration experiment on the bistable [2]rotaxane in this solvent mixture, show (Figure S13) a decrease in the fluorescence upon addition of the oxidizing agent. This result might be, in part, related to a selective solvation effect of the bistable [2]rotaxane in the binary solvent system.

Captions to Schemes and Figures

Scheme 1. (a) Covalent-bond approach to enhancing the fluorescence of the BODIPY by introducing steric constraints on the aryl ring and dipyrrin core. Box: Structure of the BODIPY-rotor employed as a viscosity sensitive probe. (b) Mechanical-bond approach to controlling the rotation of the BODIPY rotor by redox-actuation of a bistable [2]rotaxane 6^{4+}. Structural formulas and graphical representation of 6^{4+} and its redox switching from 6^{4+} to 6^{6+}.

Scheme 2. Synthesis of the BODIPY-alkyne **4**, the bistable [2]rotaxane **6**•4PF$_6$ and the dumbbell **DB**.

Figure 1. ^{1}H NMR spectra (600 MHz, CD$_3$CN, 298 K) of bistable [2]rotaxane **6**•4PF$_6$.

Figure 2. ^{1}H NMR spectra (600 MHz, CD$_3$CN, 298 K) of the bistable [2]rotaxane **6**•4PF$_6$, fully oxidized 6^{6+} after addition of 2 equiv of the chemical oxidant tris(4-bromophenyl)ammoniumyl hexachloroantimonate, and re-reduced 6^{4+} after the addition of Zn dust. Resonances due to the chemical oxidant and residual solvent are marked with red (X) symbols.

Figure 3. UV/Vis absorption spectra of a-b) the bistable [2]rotaxane **6**•4PF$_6$ and c-d) the reference dumbbell **DB** in MeCN (6.25 µM, 10 mm optical pathway) following addition of Fe(ClO$_4$)$_3$ as the chemical oxidant.

Figure 4. Cyclic voltammograms of (a) the ring component **CBPQT**•4PF$_6$, (b) the BODIPY-alkyne **4**, (c) the dumbbell **DB** and (d) the bistable [2]rotaxane **6**•4PF$_6$.

Figure 5. DFT Calculated relative energy surface diagram of a) 6^{4+} and b) 6^{6+}. Compound 6^{4+} exists as a single ground state co-conformation that may be switched wholly to its inverse state as a result of a translation of the CBPQT^{4+} ring on the TTF-containing dumbbell unit to afford 6^{6+}, where the CBPQT^{4+} ring is located on BODIPY unit as a consequence of Coulombic repulsions originating from the TTF^{2+} unit.

Figure 6. Fluorescence spectral changes of the bistable [2]rotaxane **6**•4PF$_6$ (green traces) in a) PhMe, b) THF, and c) MeCN following addition of 1 equiv (orange traces) and 2 equiv (red traces) of Fe(ClO$_4$)$_3$ as the chemical oxidant.
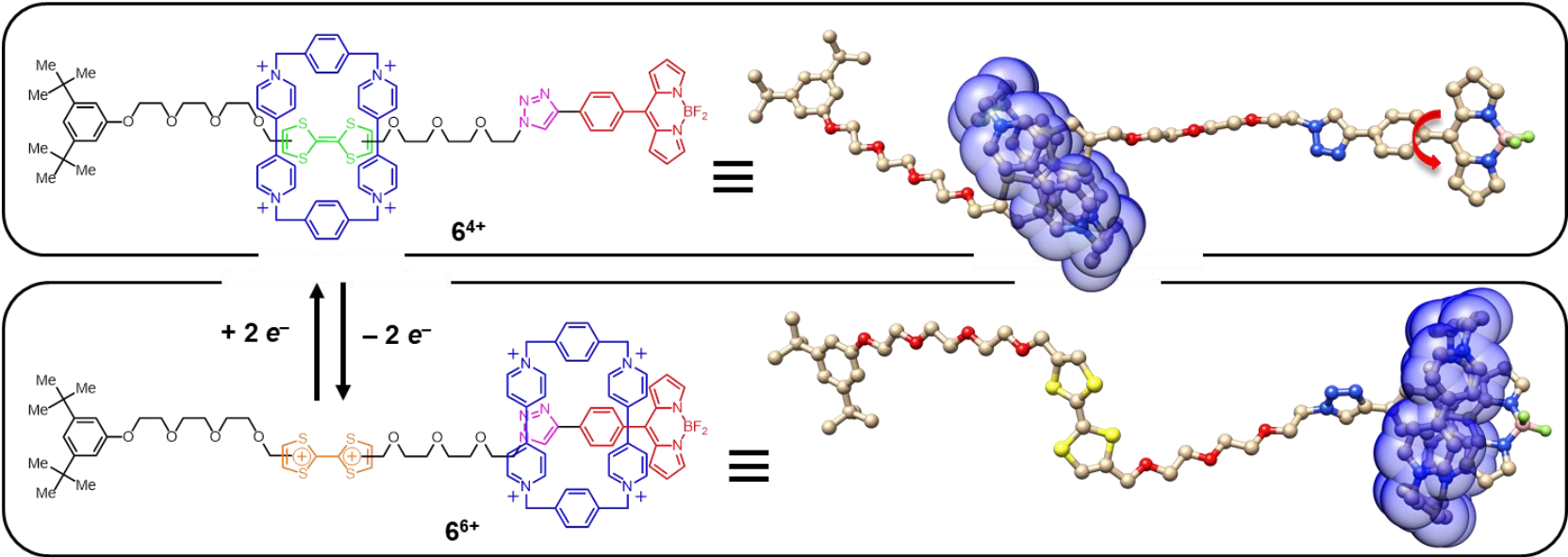
Figure 7. fsTA spectroscopy of the bistable [2]rotaxane **6**•4PF$_6$ in MeCN a-b) before and c-d) after addition of 2 equiv of Fe(ClO$_4$)$_3$ as the chemical oxidant. Samples were excited at 497 nm with a ~150 fs laser pulse. a,c) fsTA spectra at selected delay times; b,d) kinetic fits at selected wavelengths.

Figure 8. Energy diagram showing excited state decay pathways of the bistable [2]rotaxane **6**•4PF$_6$ in MeCN a) before and b) after the addition of 2 equiv of Fe(ClO$_4$)$_3$ as the chemical oxidant. In the low polarity solvent such as PhMe (c), the photoinduced electron-transfer reaction is energetically unfavorable and the fluorescence decay enhances on account of hindered intramolecular rotation responsible of nonradiative decay process.

a) Covalent-Bond Approach
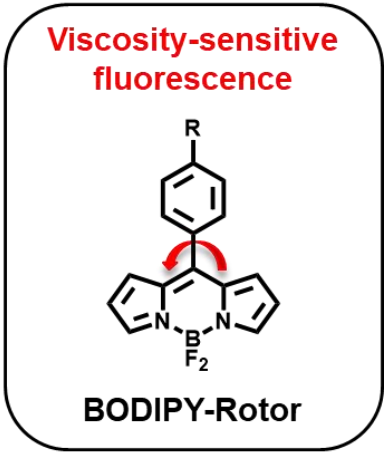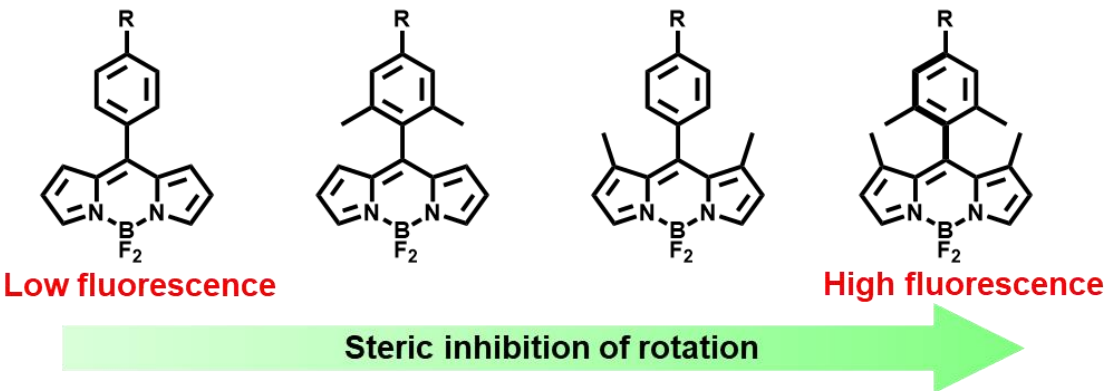
Low fluorescence

Steric inhibition of rotation

High fluorescence

Viscosity-sensitive fluorescence

BODIPY-Rotor

b) Mechanical-Bond Approach

6^{4+}

$+ 2 e^-$ $- 2 e^-$

6^{6+}

≡

Scheme 1

Scheme 2
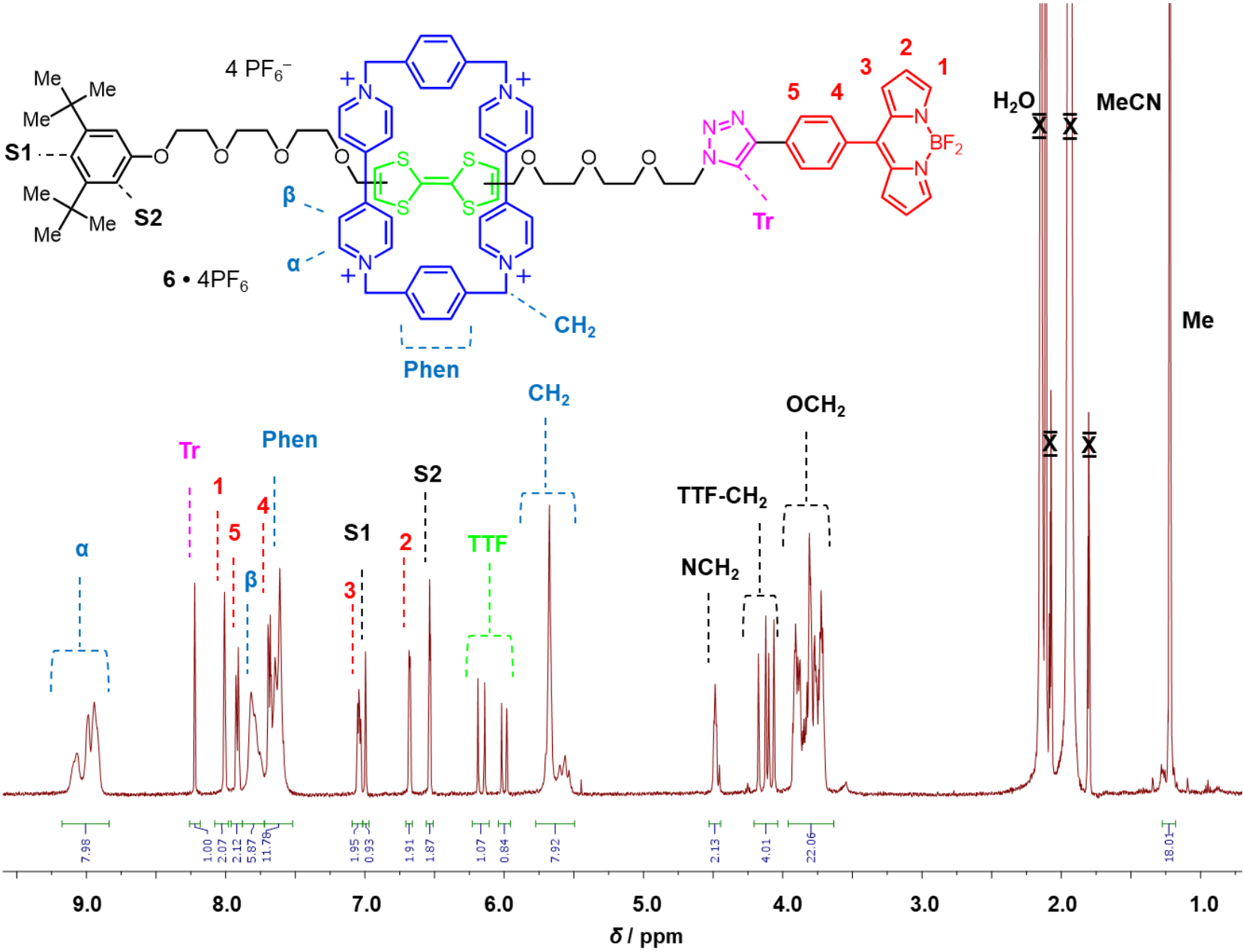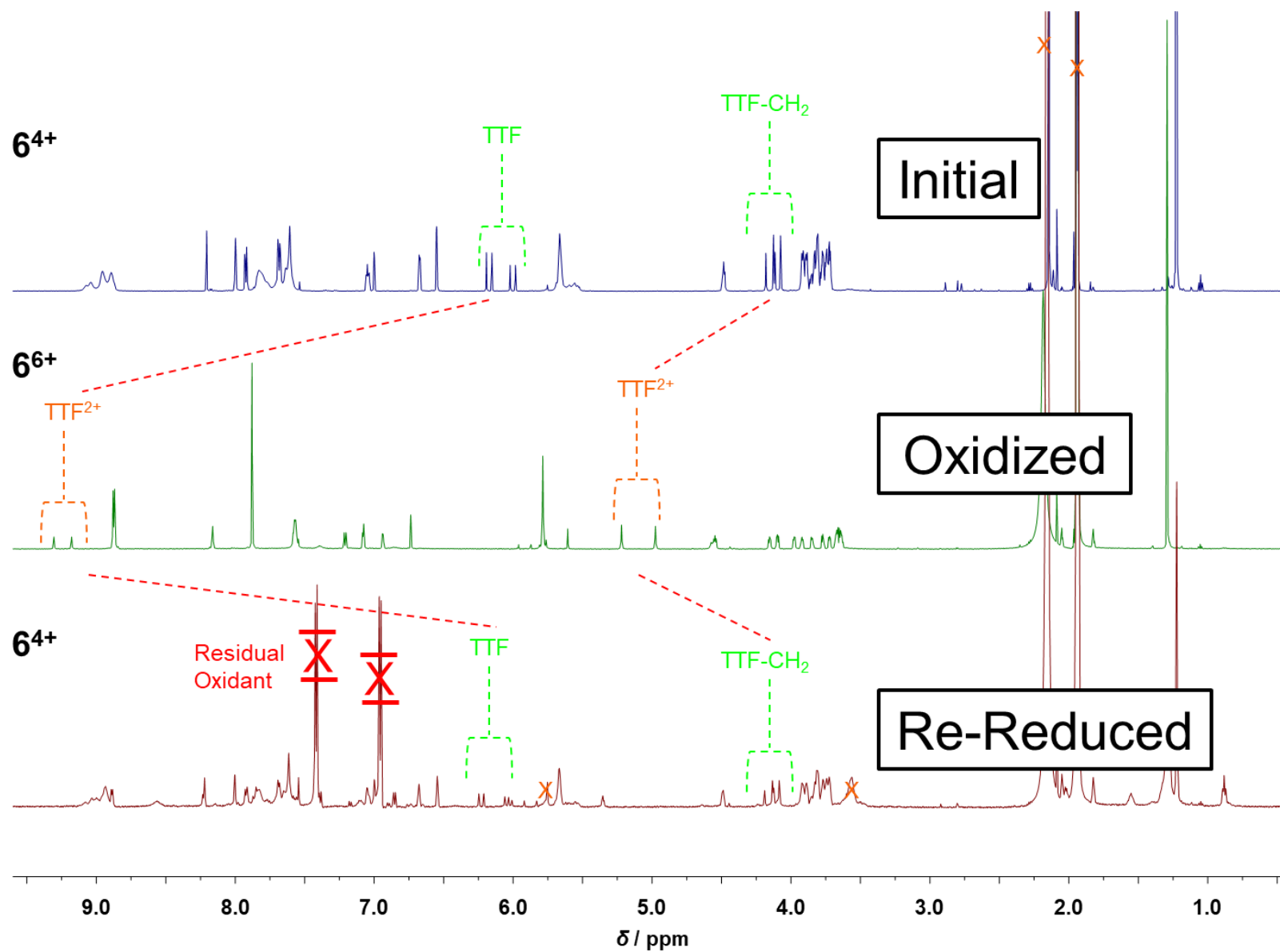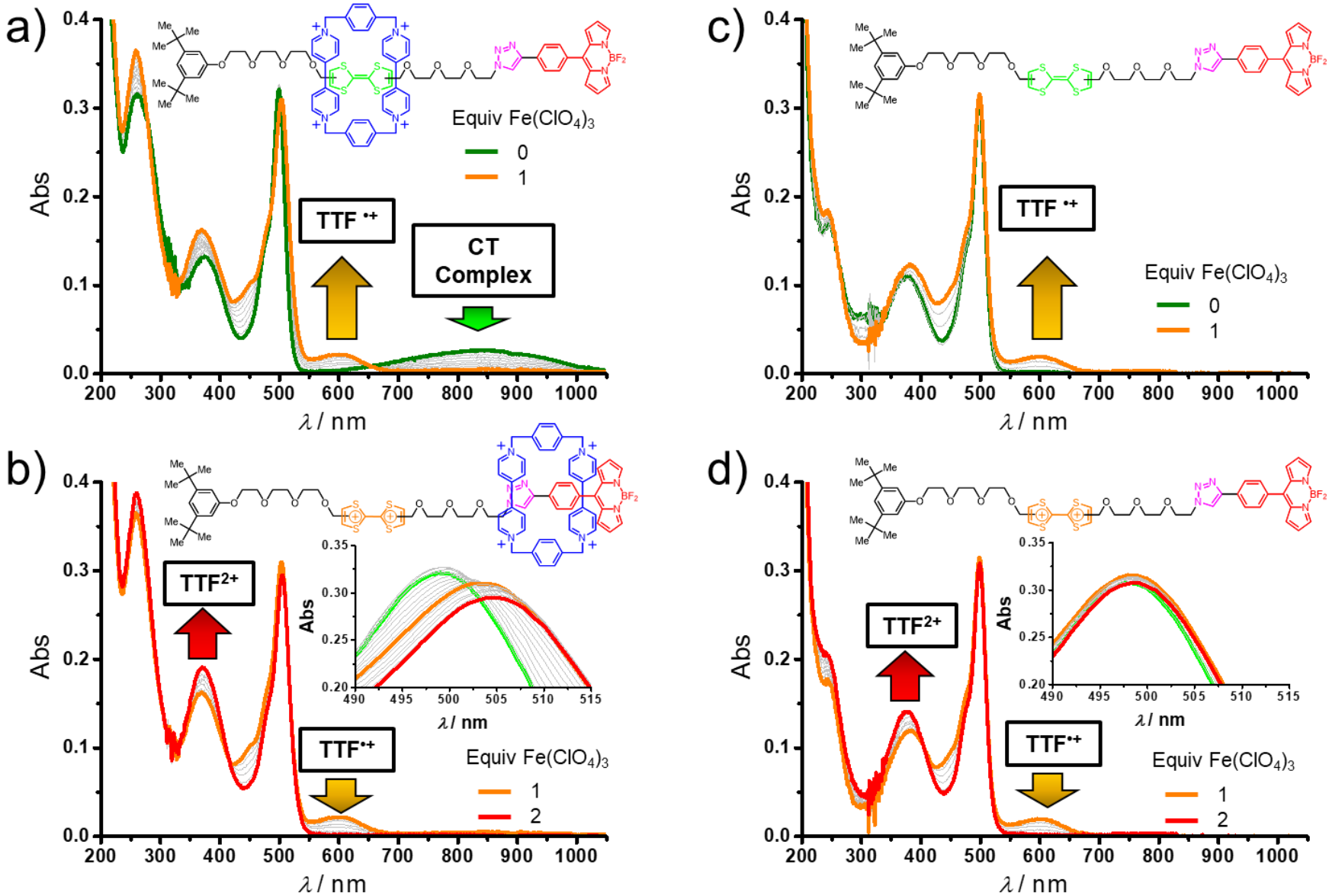
Figure 1

Figure 2
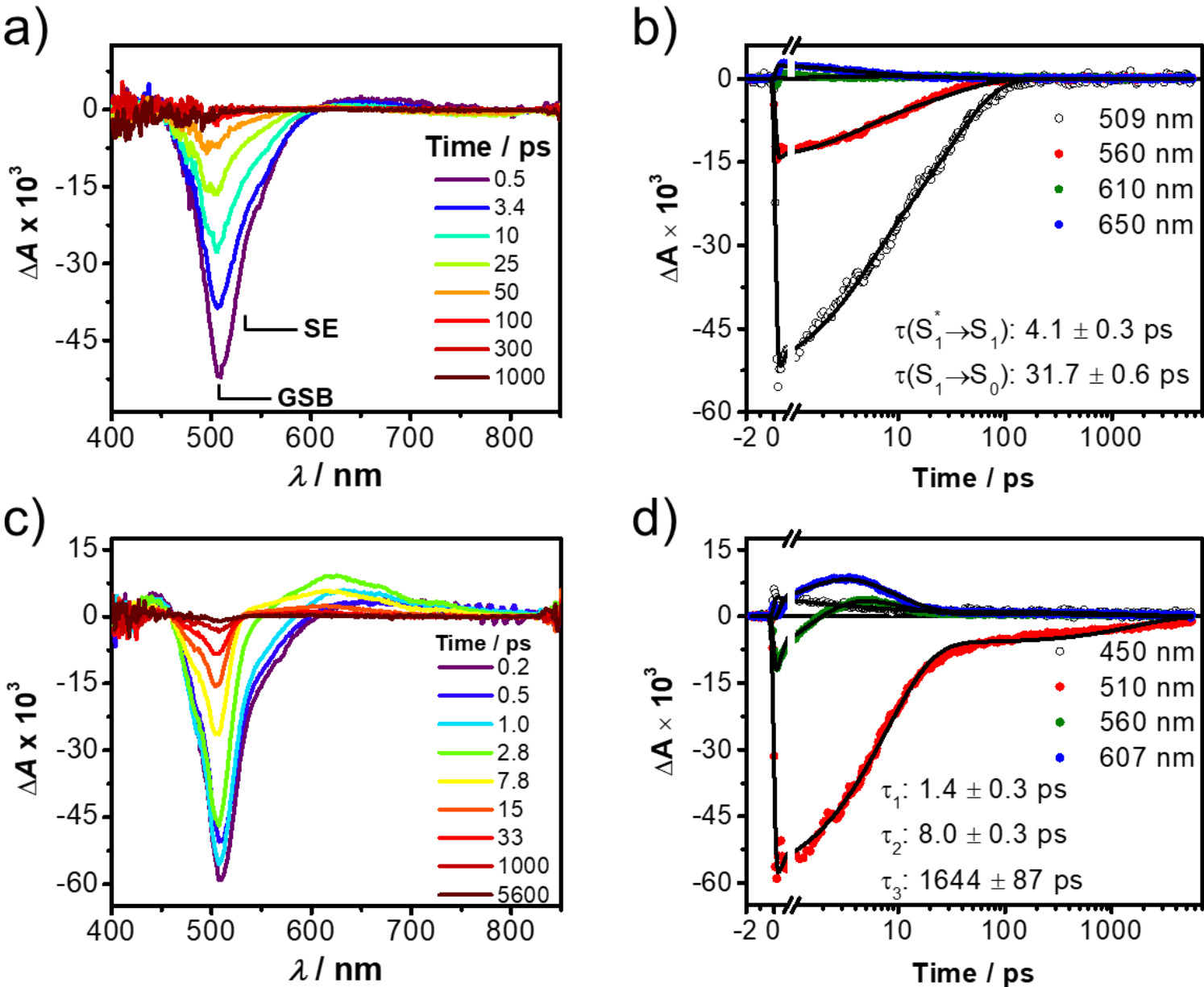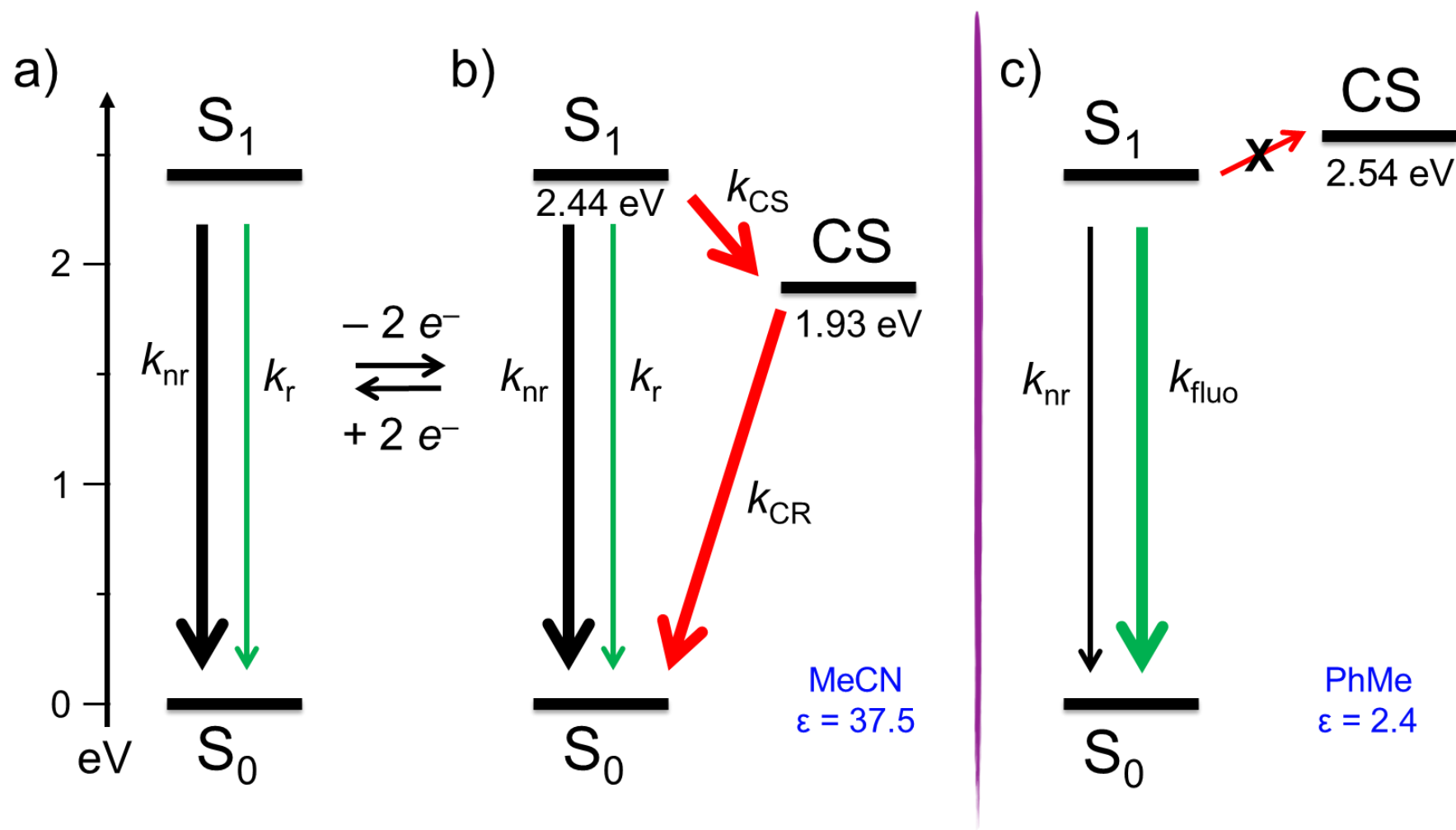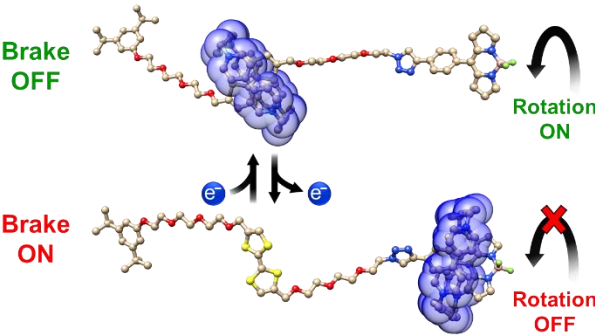
Figure 3
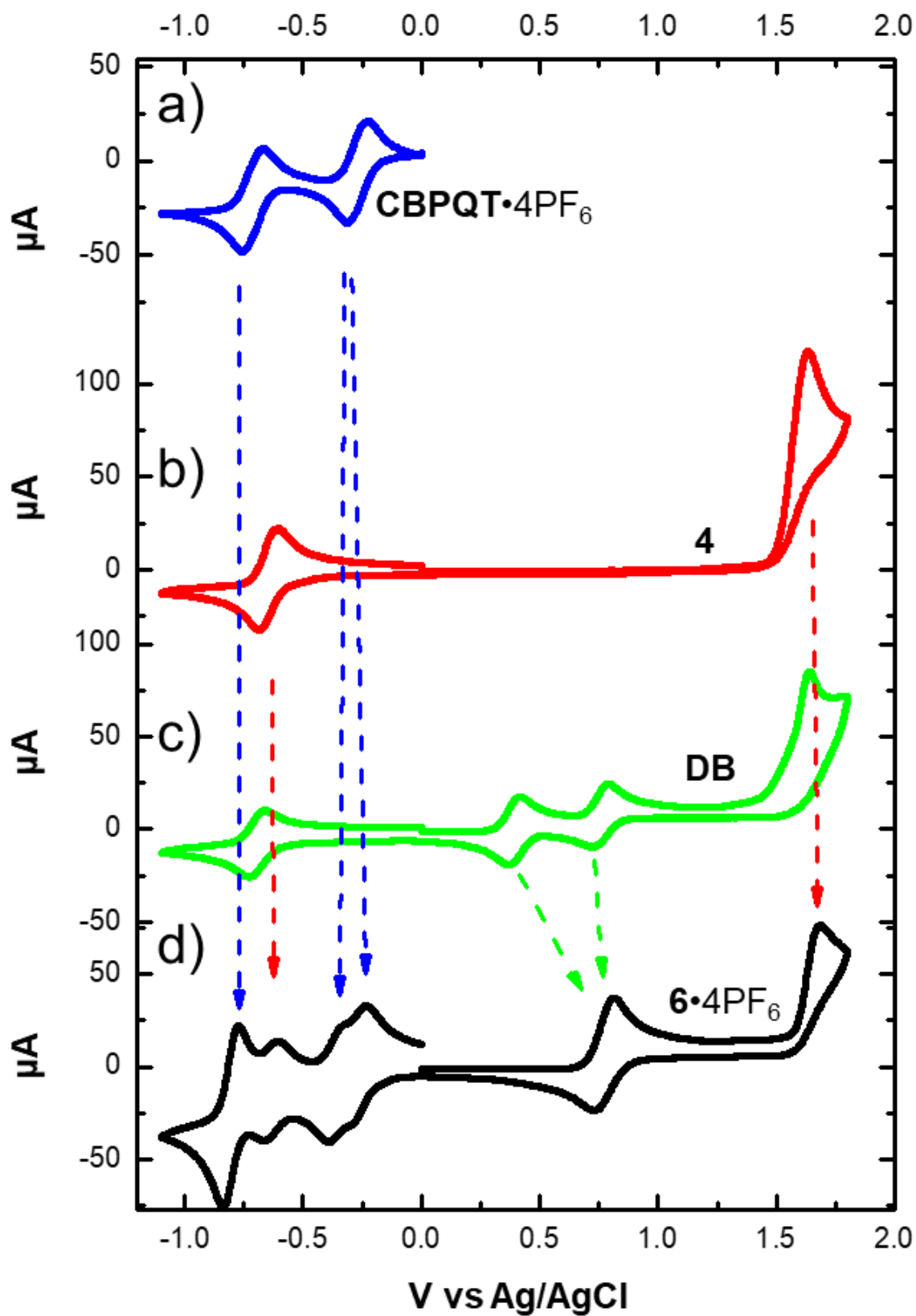
Figure 4
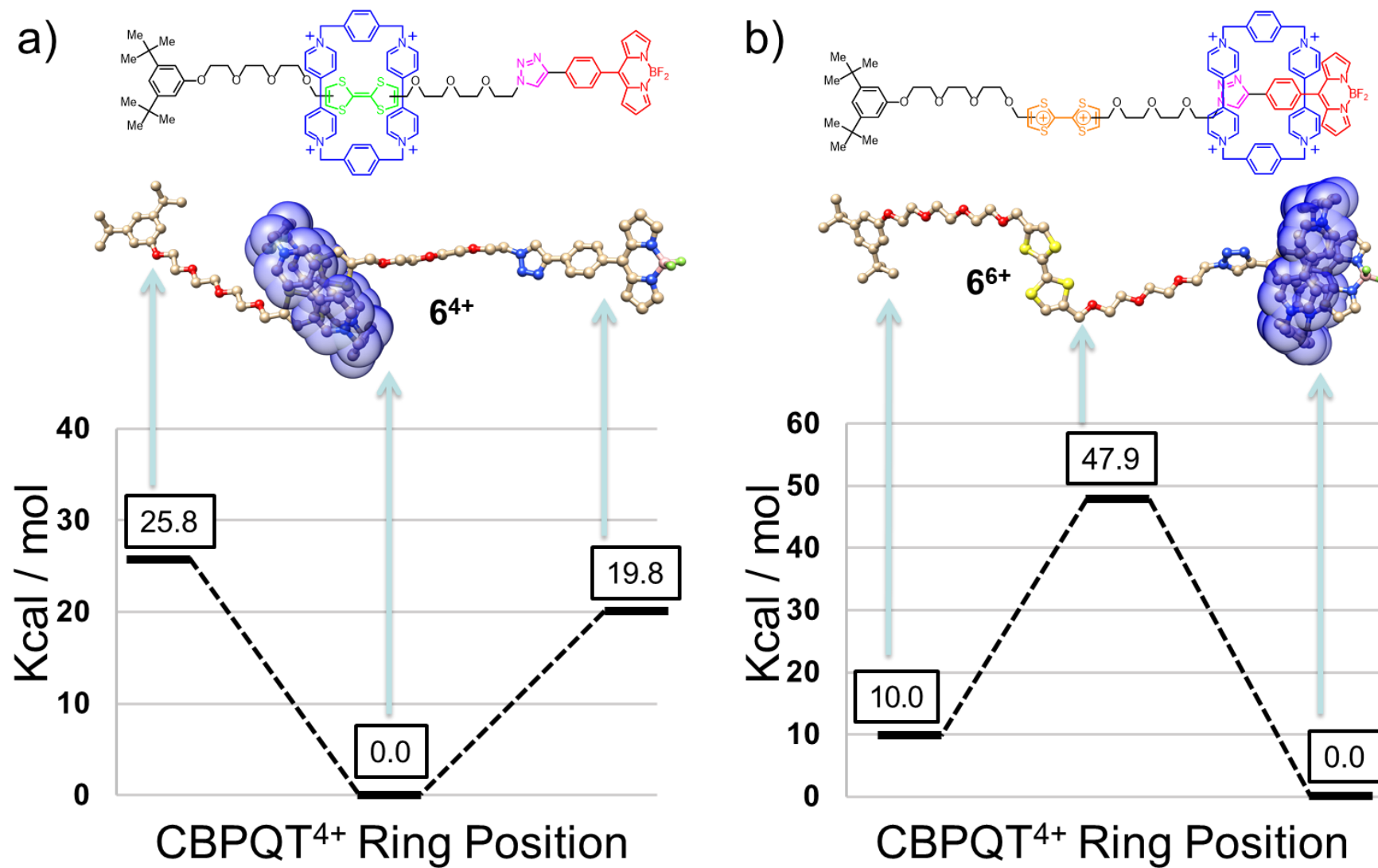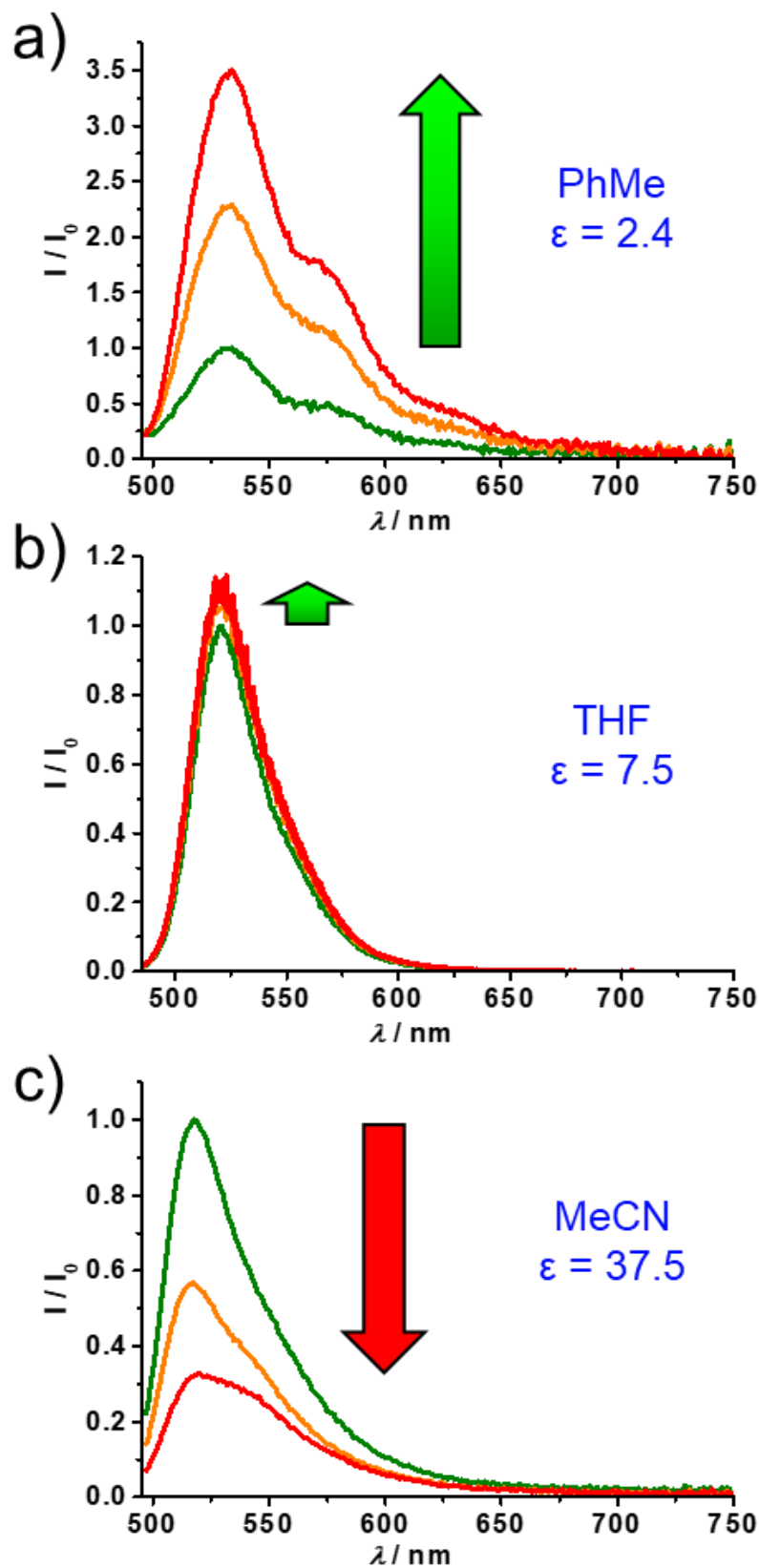
Figure 5

Figure 6

Figure 7

Figure 8

For Table of Contents Only